Published in final edited form as:
Dev Biol. 2009 April 1; 328(1): 160–172. doi:10.1016/j.ydbio.2009.01.024.

Bicaudal-C Associates with a Trailer Hitch/Me31B Complex and is Required for Efficient Gurken Secretion

Jan-Michael Kugler[‡], **Jarred Chicoine**[‡,1], and **Paul Lasko**[*]
Department of Biology, McGill University, 1205 Avenue Docteur Penfield, Montréal, Québec, Canada H3A 1B1

Abstract

Bicaudal-C (Bic-C) is a multiple KH-domain RNA-binding protein required for *Drosophila* oogenesis and, maternally, for embryonic patterning. In early oogenesis, Bic-C negatively regulates target mRNAs, including *Bic-C*, by recruiting the CCR4 deadenylase through a direct association with its NOT3 subunit. Here, we identify a novel function for Bic-C in secretion of the TGF-α homolog Gurken (Grk). In *Bic-C* mutant egg chambers, Grk is sequestered within actin-coated structures during mid-oogenesis. As a consequence, Egfr signalling is not efficiently activated in the dorsal-anterior follicle cells. This phenotype is strikingly similar to that of *trailer hitch* (*tral*) mutants. Consistent with the idea that Bic-C and Tral act together in Grk secretion, Bic-C co-localizes with Tral within cytoplasmic granules, and can be co-purified with multiple protein components of a Tral mRNP complex. Taken together, our results implicate translational regulation by Bic-C and Tral in the secretory pathway.

Introduction

The anterior/posterior (A/P) and dorsal/ventral (D/V) axes of the future embryo are both established during *Drosophila* oogenesis by signalling events between the oocyte and the overlying somatic follicle cells. These signals are mediated in part by the TGF-α homologue Gurken (Grk), which is secreted from the oocyte to activate the follicle cell-bound Epidermal Growth Factor receptor (Egfr) (Gonzalez-Reyes *et al*., 1995). This initially occurs at stage 6, when activation of Egfr in a posterior group of follicle cells triggers the production of an unknown signal that establishes the A/P axis of the oocyte. As a consequence, the microtubule cytoskeleton reorganizes within the oocyte such that patterning determinants localize to distinct sub-cellular domains. The oocyte nucleus, which is closely associated with *grk* mRNA throughout most of oogenesis, migrates to the anterior cortex in response to the cytoskeletal rearrangements at stage 7. Localized Grk then specifies the dorsal side of the oocyte through a second round of Egfr activation in the anterior/lateral follicle cells that are adjacent to the oocyte nucleus (Neuman-Silberberg and Schüpbach, 1993).

Grk is cleaved in the ER by the membrane-bound protease Rhomboid 2, to produce the active, secreted form, which is then tethered by Cornichon (Cni) (Ghiglione *et al*., 2002; Guichard *et*

*Corresponding Author tel 1 514 398 6401, fax 1 514 398 5069, e-mail E-mail: paul.lasko@mcgill.ca.
‡Equal Contribution
[1]Present address: Department of Human Genetics, McGill University and Genome Quebec Innovation Centre, 740 Avenue Docteur Penfield, Montréal, Québec, Canada, H4A 1A4

al., 2000). Cni is a transmembrane protein that acts as a cargo receptor, recruiting Grk into COPII-coated vesicles for rapid export (Guichard *et al*., 2000). An ER-associated ribonucleoprotein (RNP) complex, containing Trailer Hitch (Tral), Maternal Expression at 31B (Me31B), Ypsilon Schachtel (Yps), Poly(A) Binding Protein (PABP) and Cup, has been implicated in the maintenance of COPII exit sites from the ER and consequently for efficient exocytosis of Grk and other secreted proteins during oogenesis (Wilhelm *et al*., 2005).

Me31B is a DDX6-like DEAD-box ATP-dependent RNA helicase that localizes to maternal RNPs called sponge bodies, where it is required for translational silencing of multiple mRNAs including the pole plasm determinant *oskar* (Nakamura *et al*., 2001). Me31B also co-localizes with the mRNA decapping factors DCP1 and DCP2 in cytoplasmic foci resembling processing bodies (P-bodies) (Lin *et al*., 2006). P-bodies are sites of mRNA storage and/or decay, defined by the absence of ribosomes and translation factors (with the exception of eIF4E) and the presence of several proteins involved in mRNA degradation including DCP1 and DCP2, the 5'-3' exonuclease XRN1, and the deadenylase CCR4 (Anderson and Kedersha, 2006). Orthologues of Me31B in *S. cerevisiae* (Dhh1), *C. elegans* (CGH-1), *X. laevis* (Xp54) and mammals (RCK/p54), are also components of P-bodies and/or contribute to translational silencing of maternal mRNAs (Weston and Sommerville, 2006). Likewise, the human orthologue of Tral, RAP55, is a component of P-bodies and plays a critical role in their assembly (Yang *et al*., 2006). Like Me31B, both Xp54 and CGH-1 associate with the respective Yps and Tral orthologues in *X. laevis* and *C. elegans* respectively, indicating that these proteins operate within an evolutionarily conserved complex that likely performs similar functions in divergent metazoan species (reviewed by Weston and Sommerville, 2006).

Me31B was recovered in a yeast-two-hybrid screen for Bicaudal-C (Bic-C) interacting proteins (Chicoine *et al*., 2007). Bic-C is a KH-type RNA-binding protein that acts antagonistically to the CPEB-like protein Orb to regulate cytoplasmic movements during oogenesis, through recruitment of the CCR4-POP2-NOT deadenylase complex to target transcripts (Chicoine *et al*., 2007). Like Me31B and Cup, Bic-C is also required for translational repression of unlocalized *oskar* and consequently anterior/posterior embryonic patterning (Nakamura *et al*., 2001; Wilhelm *et al*., 2005; Saffman *et al*., 1998).

We report here that Bic-C associates with Me31B, Tral, PABP and Cup during oogenesis and that, like Tral, Bic-C is required for efficient Grk secretion.

Results

Bic-C and *cni* interact genetically

Bic-C mutant females display a haplo-insufficient maternal effect phenotype in which a small percentage of the offspring embryos show variable deformations that range from mild segmentation defects to fully bicaudal (Mahone et al., 1995). As a consequence, a proportion of these embryos fail to hatch into larvae. This phenotype is consistently more severe when the mutant *Bic-C* allele is maternally derived (compare the heterozygous *Bic-C* flies in Table 1 and Table 2). A screen for dominant enhancers of this phenotype revealed a strong genetic interaction between *Bic-C* and *cni* (Table 1). Embryos derived from females bearing a mutant allele of *Bic-C* in trans to an allele of *cni* display a synergistic reduction in viability as compared to embryos produced by females mutant for only a single allele.

Gurken accumulates ectopically in *Bic-C* mutant oocytes

Because Cni is the cargo receptor for Grk during secretion (Guichard et al., 2000), the genetic interaction between *Bic-C* and *cni* led us to hypothesize that Bic-C might be involved in Grk secretion. To test this, we monitored Grk distribution in wild-type (wt) and *Bic-C* mutant

ovaries (Fig. 1). In wt oocytes, Grk protein begins to accumulate at the anterodorsal cortex, in close association with the oocyte nucleus, at stage 7, where it remains through late stage 9 (Fig. 1A). Virtually no Grk is observed on the side of the oocyte nucleus which faces the center of the oocyte. In clear contrast, Grk distribution is significantly altered in *Bic-C* mutant egg chambers during mid-oogenesis (Fig. 1B). In *Bic-C* oocytes, Grk is not restricted to the anterodorsal cortex, but surrounds the entire oocyte nucleus, clustered in spheroid aggregates that also face the center of the oocyte.

grk mRNA localization is a highly regulated process, and is a prerequisite for restricted local secretion of Grk protein to the anterodorsal follicle cells (Herpers and Rabouille, 2004). To ascertain whether aberrant *grk* mRNA localization might be the cause of the abnormal distribution of Grk protein in *Bic-C* mutants, we simultaneously visualized *grk* mRNA and Grk protein. Both in wt and in *Bic-C* mutant egg chambers, *grk* mRNA is closely associated with the oocyte nuclear membrane at stage 9 (Fig. 1A, B). However, in *Bic-C* mutants *grk* mRNA is concentrated primarily between the nucleus and the anterior cortex of the oocyte.In wt oocytes, *grk* mRNA is primarily enriched along the dorsal cortex, with less enrichment adjacent to the nuclear membrane, closely mirroring the distribution of Grk protein. Thus Bic-C may be involved in fine-tuning of the *grk* mRNA localization pattern. In *Bic-C* mutant oocytes we observe only a partial overlap between Grk protein and the site of transcript accumulation, in that Grk protein accumulates in spheres that can be quite distant from the site of *grk* mRNA accumulation. This supports the idea that a defect occurring after translation is the major underlying cause of the abnormal Grk distribution in *Bic-C* mutant oocytes.

Grk signaling is impaired in *Bic-C* oocytes

We next asked whether activation of the epidermal growth factor receptor (Egfr) is compromised in *Bic-C* egg chambers. We compared expression of *mirr-lacZ*, a marker for Egfr activation in the anterodorsal follicle cells (Zhao *et al*., 2000), in ovaries either heterozygous or homozygous for the strong *Bic-C*^{YC33} allele. Immunofluorescent labelling demonstrates that in *Bic-C* heterozygotes, Grk distribution and *mirr-lacZ* expression are indistinguishable from wt (Fig. 1C and data not shown). However, in homozygous *Bic-C*^{YC33} ovaries, *mirr-lacZ* expression is greatly reduced (Fig. 1D). Therefore, the unusual distribution of Grk in *Bic-C* oocytes correlates with a failure to efficiently activate Egfr signalling. We consider it unlikely that this results from the small effect of *Bic-C* mutations on *grk* mRNA localization, as mutations in *K10*, *squid* and *Hrb27C* all cause more profound disruptions of *grk* mRNA localization, yet do not block secretion of active Grk to the follicle cells (Forlani *et al*., 1993; Goodrich *et al*., 2004).

An essential step in Grk signalling is cleavage in the ER, by the combined activities of *Star* and *stet* (also called *rhomboid-2*) (Ghiglione *et al*., 2002; Bokel *et al*., 2005). To determine whether lack of Bic-C blocks this processing step, we expressed a Myc-tagged version of Grk in wt and *Bic-C*^{YC33} homozygous ovaries (Ghiglione *et al*., 2002). Western blotting demonstrates the presence of both the uncleaved Grk species as well as of the C-terminal cleavage remnant both in wt and *Bic-C*^{YC33} ovaries (Fig. 1E). This indicates that the failure to activate Egfr in the dorsoanterior follicle cells is not caused simply by a defect in Grk cleavage.

Mislocalized *Grk* accumulates in F-actin coated spheres

To further characterize the nature of the ectopic Grk foci, we labeled wt and *Bic-C* mutant egg chambers with Rhodamine-Phalloidin to visualize the F-actin cytoskeleton. In wt oocytes, F-actin is predominantly found in tight association with the cell membranes (Fig. 2A, B). In contrast, cortical F-actin often appears disorganized in *Bic-C* mutant oocytes and, unlike in wt controls, the oocyte frequently separates from the overlying follicle cells during fixation and staining (Fig. 2C-E). *Bic-C* mutant oocytes additionally display spherical F-actin-coated

structures which are detectable as early as stage 6. These spheres are initially found primarily along the anterior margin of the oocyte. The structures increase both in size and number until egg chambers cease developing at stage 10b and subsequently degenerate. Many of the F-actin-coated spheres cluster around the oocyte nucleus. Although the migration of the oocyte nucleus to the anterior/dorsal cortex at stage 7/8 occurs normally in *Bic-C* mutants, the oocyte nucleus is frequently found dissociated from the anterior cortex during stages 9-10 (Fig. 2E). In these cases, many spheroid F-actin structures remain closely associated with the detached nucleus.

We have observed similar structures and ectopic Grk accumulation in several independently derived *Bic-C* mutants (data not shown). Furthermore, germline-specific expression of TAP-tagged Bic-C (pUASP-TAP-Bic-C) prevents the accumulation of actin-coated structures within the oocyte and rescues the centripetal follicle cell migration defect characteristic of *Bic-C* mutants (Fig. 2F-H). These results confirm that lack of *Bic-C* activity in the germline underlies the defects in microfilament organization in *Bic-C* oocytes.

Importantly, the F-actin spheres and the sites of ectopic Grk accumulation overlap (Fig. 2I). Ectopic Grk foci facing the center of the oocyte are always encapsulated by F-actin. However, many of the F-actin spheres do not contain Grk, especially those that are more distant from the oocyte nucleus. This argues that the ectopic accumulation of Grk is not the primary cause for the formation of the F-actin coated structures.

F-actin coated spheres in *Bic-C* egg chambers contain a distinct set of secretory proteins

The accumulation of Grk within F-actin coated spheres in *Bic-C* mutant oocytes suggests that Grk might be trapped in an aberrantly acting secretory compartment through which proteins cannot transit. In this case, the F-actin spheres should include a distinct subset of proteins that function in the exocytic pathway. The relationship between Bic-C and Tral (discussed below) prompted us to initially focus on markers for the endoplasmic reticulum (ER). We imaged fixed and live *Bic-C* mutant egg chambers (and heterozygous control siblings) expressing available GFP protein traps (Buszczak et al., 2007; Lighthouse et al., 2008) that reveal the distribution of the translocon complex (Sec63-GFP), ER chaperone proteins [disulfide isomerase (PDI-GFP) and calreticulin (Crt-GFP)], ER membranes (Surf4-GFP), and COPII exit sites (Sar1-GFP) (Wilhelm et al., 2005); and we additionally performed immunocytochemistry using antibodies specific for the ER chaperones BiP and calnexin (Cln) and the ER resident protein Boca (Culi and Mann, 2003).

During mid-oogenesis, we observed essentially no germ line expression of Surf4-GFP while we observed a prominent signal in the follicular epithelium and in the border cells (data not shown). We therefore did not further analyze this marker. In fixed ovary samples, Sec63-GFP, PDI-GFP and Crt-GFP all form a particulate pattern throughout wt oocytes (Fig. 3 and data not shown). In fixed *Bic-C* mutant egg chambers, this pattern is not substantially altered. We did not observe enrichment of these markers within the actin-coated spheres; in fact, the signal intensity for these markers was often diminished within the actin-coated spheres (Fig. 3B; and data not shown). Only Crt-GFP was occasionally present in the actin-coated structures during mid-oogenesis (Fig. 3C, D). The exclusion of Sec63-GFP, PDI-GFP, and Crt-GFP from the F-actin coated spheres was confirmed by live imaging, where we observed prominent spherical gaps in the distribution of all three markers in a *Bic-C* mutant background (Fig. 3F, H and data not shown). We believe these gaps correspond to the actin-coated structures because they initially form in the anterior of the oocyte, increase in size as oogenesis progresses and frequently remain tightly associated with the detaching oocyte nucleus. The distribution of Crt-GFP differed somewhat from those of Sec63-GFP and PDI-GFP in that the former frequently decorated spheroid structures at the posterior of *Bic-C* oocytes that we did not observe in wt egg chambers or with any other GFP markers that we utilized. Given their location, these Crt-GFP positive structures are unlikely to correspond to the actin spheres. Very rarely, Sec63-

GFP formed bright foci in the anterior of younger *Bic-C* mutant oocytes (data not shown). The ER luminal protein Boca also forms a particular meshwork throughout the oocyte cytoplasm with some cortical enrichment (Fig. 3I). In Bic-C mutant egg chambers, this pattern is not strongly altered (Fig. 3J) and Boca is neither enriched within nor excluded from the actin spheres.

The COPII exit site marker Sar1-GFP displayed a distribution pattern that was strikingly different in control and *Bic-C* oocytes. In heterozygous control oocytes, Sar1-GFP shows a particulate distribution with some cortical enrichment (Fig. 4A, C). In *Bic-C* mutant oocytes, however, Sar1-GFP accumulates in foci that are located at the anterior cortex near the nucleus (Fig. 4B, D). As egg chambers mature, these foci become more prominent and increase in size and number near the anterior of the oocyte, while additional smaller Sar1-GFP foci are observed throughout the oocyte cytoplasm at higher levels than in control egg chambers. Since the size, appearance and localization of these large Sar1-GFP foci closely resemble the F-actin-coated structures, we stained fixed samples with Rhodamine-Phalloidin to determine if they co-localize. While much of the Sar1-GFP signal was lost upon fixation, a clear enrichment of Sar1-GFP in and around the F-actin-coated structures is nevertheless visible (Fig. 4E, F). In contrast to PDI-GFP and Crt-GFP, we observed a substantial enrichment of the ER chaperones BiP and Cln in the actin-coated structures in *Bic-C* oocytes (Fig. 5). α-BiP and α-Cln produce a particulate staining pattern throughout wt oocytes that is enriched around the cortex (Fig. 5A, C). In *Bic-C* mutant oocytes, however, these two markers are also clearly concentrated within the lumen of the actin spheres (Fig. 5B, C).

In summary, the actin coated spheres contain Boca and are enriched for COPII exit sites and for the ER chaperones BiP and Cln. They however exclude other ER chaperones (PDI-GFP and Crt-GFP) and the translocon complex component Sec63-GFP. This is consistent with a defect in ER exit site formation in *Bic-C* mutants that affects a specific subset of cargo vesicles destined for transport to the Golgi. However, if the requirement for *Bic-C* activity is limited to ER exit site formation, the actin spheres would be predicted not to contain markers that characterize downstream membrane compartments in the secretory pathway. To test this, we immunolabelled *Bic-C* heterozygous and homozygous ovaries with an antibody raised against a conserved sequence in the KDEL receptor (KDEL-R) which is enriched at steady state in the *cis*-Golgi apparatus and mediates retrograde transport of KDEL-containing proteins from the Golgi to the ER (Pfeffer, 2007). In control egg chambers, α-KDEL-R produces a particulate staining pattern throughout the cytoplasm of the oocyte and the nurse cells (Fig. 5E). In addition, it labels structures within the nurse cell nuclei which we assume to result from cross-reactivity. In *Bic-C* mutant oocytes, however, α-KDEL-R signal is highly enriched within and near the actin-coated spheres (Fig. 5F), indicating that this *cis*-Golgi marker, like the ER markers discussed above, is associated with these structures. We also labelled ovaries with an antibody which detects the *cis*-Golgi marker protein GM130 (abcam; Barr and Short, 2003). The antibody produces a particulate staining pattern throughout the oocyte cytoplasm with cortical enrichment in both control and *Bic-C* mutant oocytes. We did not observe enrichment or exclusion of this marker from the actin spheres (data not shown).

We next immunolabelled *Bic-C* heterozygous and homozygous ovaries with antibodies that recognize Rab11 (Fig. 6A, B), which is enriched in recycling endosomes (Tanaka and Nakamura, 2008), the early endosomal marker Rab5 (Fig 6C, D), and the late endosomal marker Rab7 (Fig. 6E, F). In *Bic-C* heterozygous ovaries, all three markers are found throughout the oocyte cytoplasm, with clear enrichment at the oocyte cortex (Fig. 6A, C, E). Surprisingly, we found that Rab11 and Rab5 were enriched within and near the actin-coated spheres in *Bic-C*^{YC33} homozygous mutant ovaries (Fig. 6B, D) while Rab7 was neither enriched within, nor excluded from these structures (Fig. 6F). The distribution of the Rab5 effector Rabenosyn-5 (Tanaka and Nakamura, 2008) was largely unchanged in *Bic-C* mutant ovaries

in comparison to controls, and was not enriched or excluded from the actin spheres in most *Bic-C* egg chambers (data not shown).

Lastly, we used antibodies specific for two components of the exocyst: Sec5 and Sec8. α-Sec5 labels particulate structures throughout the oocyte cytoplasm in wild-type and heterozygous *Bic-C* ovaries (Fig. 6G; Murthy and Schwarz, 2003). However, in *Bic-C* mutant ovaries, Sec5 is strongly enriched in and around the F-actin-coated spheres (Fig. 6H). Sec8 is very strongly enriched around the lateral and posterior cortex in wild-type oocytes but is present at only low levels within the oocyte cytoplasm (Beronja et al., 2005). In *Bic-C* mutant ovaries, however, Sec8 is clearly enriched within and near the actin-coated spheres in addition to the oocyte cortex in a similar manner to Sec5 (data not shown). This indicates that the actin-coated spheres are also associated with distinct endosomal markers.

Bic-C associates with multiple components of a Trailer Hitch/Me31B complex

tral mutant egg chambers display defects in Grk secretion that are similar to those we observe in *Bic-C* mutants (Wilhelm et al., 2005). Furthermore, the identification of Me31B both as a component of a Tral mRNP complex (Wilhelm et al., 2005) and as a putative Bic-C-interacting protein (Chicoine *et al*., 2007), suggests a possible functional and physical association between Bic-C and Tral-containing mRNPs. To explore this possibility and confirm our previous findings, Me31B-eGFP (Nakamura *et al*., 2001) was immunoprecipitated from ovarian extracts with α-GFP and immune complexes were analyzed by western blotting with antibodies specific to Bic-C and Cup (Fig. 7A). While Bic-C and Cup are both specifically enriched in the Me31B-eGFP immune complex, the interaction between Bic-C and Me31B is more resistant to RNAse treatment than that of Cup and Me31B (Fig. 7A). This is consistent with the interaction between Bic-C and Me31B in the yeast-two-hybrid system (Chicoine et al., 2007) and previous observations that the Cup-Me31B interaction is RNA-dependent (Nakamura et al., 2004). We also performed a reciprocal experiment and found that Me31B-eGFP is specifically enriched in α-Bic-C immunoprecipitates (Fig. 7B). To test for an interaction between Bic-C and Tral, we used α-GFP to isolate immune complexes from Tral-GFP (Wilhelm et al., 2005) ovarian extracts (Fig. 7C). Western blotting revealed that Bic-C is specifically co-precipitated with Tral-GFP and that this interaction was not strongly affected by RNAse treatment (Fig. 7C). To determine if Bic-C associates with other components of Tral-containing RNPs, Bic-C immunoprecipitates from wt ovarian extracts were analyzed by Western blotting with antibodies specific to PABP and Cup (Nelson et al., 2004). Both proteins were specifically enriched in the Bic-C immune complex in an RNA-dependent manner (Fig. 7D). Taken together, these results demonstrate that Bic-C associates with a Tral/Me31B-containing RNP complex.

Bic-C co-localizes with Tral-GFP and Me31B-eGFP *in vivo* and both proteins display an altered distribution in *Bic-C* mutants

To gain additional evidence that Bic-C associates with Tral and Me31B *in vivo*, we immunolabelled ovaries expressing Tral-GFP or Me31B-eGFP with α-Bic-C. In wt stage 10a egg chambers, Bic-C is expressed throughout the nurse cell and oocyte cytoplasm, and is particularly concentrated into structures that demonstrate striking co-localization with Tral-GFP (Fig. 8A). These Bic-C positive structures are more prominent in Tral-GFP ovaries than in wt, suggesting that overexpression of Tral recruits additional Bic-C into them. Me31B-eGFP also accumulates in discrete cytoplasmic foci in both the nurse cells and the oocyte, which have been shown to co-localize with Tral throughout much of oogenesis (Fig. 8B, Boag *et al*., 2005). During mid-oogenesis, Bic-C is concentrated in the oocyte cytoplasm and its distribution is granular but more diffuse than that of Me31B. However, both proteins are clearly enriched together in punctate structures within the oocyte (Fig. 8B).

We next asked if the distribution of Tral-GFP is altered in the absence of Bic-C. At stage 8/9, Tral-GFP distribution in *Bic-C* heterozygotes is indistinguishable from that in wt egg chambers, where it displays punctate localization throughout the nurse cell and oocyte cytoplasm, with some slight enrichment along the anterior cortex (Fig. 8C). However, in a *Bic-C* null background, Tral-GFP is reduced in the central portion of the oocyte and is more prominently concentrated along the anterior and posterior oocyte cortex (Fig. 8D). Me31B-eGFP is similarly concentrated along the anterior and posterior cortex in the absence of Bic-C (Fig. 8F). Unlike Tral-GFP, Me31B-eGFP levels appear to be higher in the *Bic-C* null background (*Bic-C*^{YC33}/*Df2LRA5*) than in heterozygous *Bic-C*^{YC33}/+ controls (Fig. 8E, F).

Simultaneous reduction of Bic-C and Tral results in a synergistic reduction in fertility

If Bic-C and Tral function together in a complex regulating ER function during oogenesis, a concurrent reduction in the levels of both proteins might result in a synergistic reduction in fertility. To explore this possibility we generated trans-heterozygous females bearing mutations in *Bic-C* (*Bic-C*^{YC33} or *Bic-C*^{IIF34}) and either the strong hypomorphic *tral*^{1} P-element insertion or a genomic deletion of the *tral* locus (Mahone *et al*., 1995; Wilhelm *et al*., 2005). We then compared the hatching frequency of progeny from these females to heterozygous controls of either *Bic-C* or *tral* mutations alone. We found that trans-heterozygotes displayed a synergistic reduction in fertility that, depending on the allelic combination, ranged from 2 to 5.5 fold higher than the additive effects of both alleles (Table 2). Despite this evident effect on hatching frequency, we only infrequently observed strongly ventralized chorions among these progeny, suggesting that Grk secretion was not strongly perturbed, and we did not observe obvious defects in Grk localization (data not shown). Since disruptions in protein trafficking are expected to affect multiple proteins, this observation might indicate that there are other secreted maternal factors, required for producing viable oocytes, that are more limiting than Grk. Alternatively, these mutations may modestly affect the trafficking of many proteins in addition to Grk, and the collective effect of doing so may compromise oocyte viability.

Discussion

We present data indicating that loss of *Bic-C* severely affects Grk-mediated Egfr activation in the dorsoanterior follicle cells during mid-oogenesis. We find that Grk ectopically accumulates in F-actin coated spheres that aberrantly form in *Bic-C* mutant oocytes. These structures are enriched in the anterior of *Bic-C* oocytes and clearly extend beyond the area of Grk expression. This indicates that the failure to secrete active Grk is likely to be a consequence of, rather than a cause for, the formation of these actin-coated structures. The observation that the actin-coated structures are initially only found in the anterior of the oocyte correlates well with the anterior enrichment of Bic-C protein in stage 7-9 oocytes (Saffman et al., 1998). *tral* mutant egg chambers display similar defects in Grk secretion, and we provide biochemical and genetic evidence that Bic-C and Tral interact both physically and functionally. Tral has been shown to associate with *sec13* and *sar1* mRNAs which encode COPII exit site components, and *tral* mutants display ectopic accumulations of Sar1-GFP throughout the nurse cell and oocyte cytoplasm, similar to those we observe in the oocyte cytoplasm of *Bic-C* mutants (Wilhelm et al., 2005; this study). Taken together, these observations could suggest that Tral and Bic-C regulate ER exit site homeostasis and that the F-actin spheres represent an aberrantly acting exit site compartment which traps proteins, including Grk, that are destined for secretion. Importantly, the actin-coated spheres contain only a subset of ER chaperones (BiP and Calnexin) while excluding several others such as Calreticulin and PDI, suggesting distinct properties for these various chaperones. This is consistent with an earlier study indicating that Calnexin and Calreticulin have distinct activities and substrate specificities, despite their extensive similarity (Kleizen and Braakman, 2004), and further argues that secretion of only a subset of proteins exported from the ER may be compromised in *Bic-C* mutants.

We also observe strong accumulation of specific endosomal Rab proteins and the exocyst components Sec5 and Sec8 within and near the actin spheres. Consequently, it appears unlikely that Bic-C is exclusively involved in COPII exit site formation and suggests functions for *Bic-C* in other aspects of the secretory pathway. We cannot rule out, however, that a primary defect in exit site formation causes secondary perturbations in other secretory compartments.

Taken together, our analysis of markers for many different steps in the secretory process indicates that the actin-enriched spheres that are apparent in *Bic-C* mutant oocytes accumulate proteins that would be present in distinct membrane compartments in wild-type cells. Perhaps a loss of Bic-C leads to inappropriate fusion of compartments into the large actin-positive structures we observe. Alternatively, Bic-C may affect the secretory process at several distinct stages, thus causing a clustering of endomembrane structures within the actin spheres.

The pleiotropic effects of *Bic-C* on oogenesis are consistent with a widespread defect in protein secretion. Such a defect would result in a communication breakdown between the developing oocyte and the overlying follicle cells, because many signalling molecules, including Grk, would not efficiently reach their target receptors on the follicle cells, and receptors may not reach the surface of the oocyte to convey signals back to the germline. Effects on protein secretion could explain the defective centripetal follicle cell migration observed in *Bic-C* mutants (Mahone *et al*., 1995), since Saxophone, the receptor for Dpp, is required in the germline for these migratory events to occur (Twombly *et al*., 1996). Accordingly, this follicle cell migration phenotype is rescued through germline-specific expression of TAP-Bic-C, indicating that Bic-C functions non-cell autonomously in this regard. A defect in protein trafficking would also disrupt membrane growth and/or the localization of adhesion factors, causing the oocyte to detach from the overlying follicle cell layer, as we have observed in *Bic-C* mutants (see Fig. 2B and D). A similar loss of oocyte adhesion has been observed in mutants of *jagunal*, which encodes a novel ER membrane protein required for sub-cortical ER clustering during oogenesis (Lee and Cooley, 2007).

The underlying cause for the secretory defect in *Bic-C* mutants remains uncertain. Bic-C acts as a translational repressor during early oogenesis and is thought to affect expression of protein from many mRNAs. We have observed the accumulation of F-actin-coated spheres in several different *Bic-C* mutant backgrounds, including $Bic\text{-}C^{RU35}$ hemizygotes, which bear a point mutation in the third KH-domain of the protein (Saffman *et al*., 1998). This mutation weakens RNA-binding activity *in vitro* and produces a severe phenotype *in vivo* without substantially affecting the level of Bic-C expression (Saffman *et al*., 1998), supporting the idea that Bic-C regulates secretion through an effect on RNA intermediates. Intriguingly, several mRNAs that are associated with Bic-C encode proteins whose sequence indicates involvement in vesicular trafficking and/or organization of the actin cytoskeleton (Chicoine et al., 2007). For instance, *CG3279*, which was over 20-fold enriched in Bic-C immunoprecipitates over pre-immune controls, encodes a protein with a predicted V-SNARE domain, suggesting a function in mediating vesicular fusion events. Another putative Bic-C target (12-fold enrichment) is dCip4, whose mammalian homologue interacts with Cdc42, which is involved both in transport from the ER to the Golgi (Aspenström 1997; Wu et al., 2000; Nakamura et al., 2008) as well as in retrograde transport from the Golgi to the ER (Luna et al., 2002). Local regulation of actin dynamics through Cdc42 is important for vesicular transport between ER and Golgi (Stamnes, 2002). Aberrant regulation of actin dynamics associated with vesicular trafficking might explain the formation of actin-coated spheres in *Bic-C* mutants and the consequent impaired secretion of Grk. Although *sec13* or *sar1* mRNAs, putative targets of Tral, were not previously found to be enriched in Bic-C immune complexes (Chicoine et al., 2007), we cannot exclude the possibility that Bic-C regulates these transcripts in conjunction with Tral, or that it regulates other transcripts important for vesicular trafficking, independently of Tral.

Since the abnormalities in Grk localization and accumulation of actin spheres become apparent when *Bic-C* mutant egg chambers appear otherwise morphologically normal, defective microfilament organization and ER exit site formation are likely to be a cause, rather than an effect, of egg chamber degeneration. In fact, abnormal F-actin and Grk accumulation are readily detectable at stage 7 in *Bic-C* oocytes, providing the first evidence that Bic-C has a function, other than auto-regulation, prior to stage 8 when it is required to suppress Osk translation (Saffman *et al*., 1998). Interestingly, *Bic-C* is not essential for Grk signalling to the posterior follicle cells at stage 6, since anterior nuclear migration and cytoskeletal re-polarization, which are initiated by this signalling event, still occur normally in most *Bic-C* mutant egg chambers (data not shown). This is consistent with reported observations in *tral* mutants and may be due to a lower required threshold of Grk to activate Egfr (or a lower essential level of Egfr activation) in the posterior follicle cells than in the anterior/dorsal follicle cells.

A subdomain of the ER, marked by Reticulon-like 1 (Rtnl1) protein, has recently been proposed to act as a transporter and/or anchor for mRNP complexes containing translationally-repressed mRNAs during *Drosophila* oogenesis (Röper, 2007). Interestingly, Rtnl1 co-localizes with Me31B, Tral and Orb within the oocyte during mid-oogenesis (Röper, 2007), raising the possibility that Orb may operate in concert with Me31B and Tral to regulate ER dynamics. It is not known whether Orb plays a role in regulating secretion, since the strongest *orb* alleles arrest very early in oogenesis (Lantz *et al*., 1994; Christerson and McKearin, 1994). However, in weaker *orb* mutants, microtubule-dependent cytoplasmic streaming is initiated prematurely at stage 8 (Martin et al., 2003). Cytoplasmic streaming is normally restricted at this stage through cross-linking of sub-cortical arrays of microfilaments and microtubules by the actin-binding proteins Cappucino and Spire, in response to Rho1 signalling (Rosales-Nieves et al., 2006). Since Bic-C associates with Orb, and antagonizes Orb activity (Castagnetti and Ephrussi, 2003; Chicoine *et al*., 2007), it is tempting to speculate that Bic-C might act through a related mechanism in regulating microfilaments and/or secretion. Future experiments aimed at determining the effects of Orb overexpression on the ER and actin cytoskeleton, and the involvement of CCR4-mediated deadenylation on repression of Tral mRNA targets should help elucidate the mechanistic basis by which Bic-C, Tral, and associated proteins act to regulate these structures.

Methods

Microscopy

In situ hybridizations were performed as described by (Kobayashi, 1999) except that after initial fixation, samples were permeabilized and re-fixed as described in method A (without Proteinase K treatment) of Nagaso *et al*., 2001. Antibody stainings were performed as described in Hawkins *et al*., 1997 for Grk staining, except H_2O_2 treatment in methanol was omitted. Primary antibodies were used at the following concentrations: α-Bic-C, 1:1000; α-Grk, 1:1000; α-β-gal (Sigma), 1:1000; α-Calnexin (Abcam), 1:400; α-BiP (Imgenex) 1:250; α-Boca, 1:500; α-Sec5, 1:35; α-Sec8, 1:2000; α-Rab5, 1:1000; α-Rab7, 1:3000; α-Rab11, 1:8000; α-Rabenosyn-5, 1:5000; α-KDEL receptor (Calbiochem) 1:1000; α-GM130 (abcam) 1:1000. Primary antibodies were detected using Alexafluor-488, -555, or -596 conjugated antibodies, 1:500 (Molecular Probes), after overnight pre-adsorption to wt ovaries. DNA and F-actin were visualized by DAPI and rhodamine-phalloidin (Molecular Probes) staining respectively. GFP-tagged proteins were either fixed for 5-10 min in 4% Formaldehyde in PBS, extensively rinsed with PBS, 0.3% Triton and counterstained with rhodamine-phalloidin, or dissected into FCS-supplemented Schneider's S2 cell medium and imaged immediately. Confocal images were acquired using a Zeiss LSM-510 microscope.

Western blots

Western blotting was performed using standard methods (Sambrook and Russell, 1989). Immunoreactive proteins were detected by chemiluminescence (NEN or Perkin Elmer). Dilutions of primary antibodies were as follows: α-Myc (Invitrogen), 1:1000; α-GFP (clones 7.1/13.1, Roche), 1:1000; α-Cup, 1:2500; α-PABP, 1:1000, α-Tral 1:2000.

Immunoprecipitations

Bic-C was immunoprecipitated from Me31B-GFP expressing ovarian extracts using the method described in Wilhelm *et al*., 2000, except that extracts were pre-cleared against protein-A Sepharose (Pharmacia) for 60 min at 4 °C, and after washing, bound proteins were eluted by boiling in Laemmli sample buffer. For every 10 mg of soluble ovarian protein extract, 80 μl of α-Bic-C sera or pre-immune sera (from the same rabbit) was used. The other immunoprecipitations were performed as follows: dissected and flash-frozen ovaries were homogenized in either mRIPA (for the Tral-GFP IPs: 10mM Tris, pH8.0; 150 mM NaCl; 2% Triton X-100; 1% sodium deoxycholate; 0,1% Nonidet P40 substitute (Fluka); 0.1% SDS; 1 mM PMSF and 1 tablet of EDTA-free protease inhibitor cocktail (Roche) per 50ml buffer) or mDXB (for the Me31B-GFP IPs and the Bic-C IPs: 25 mM HEPES, pH 6.8; 50 mM KCl; 1 mM $MgCl_2$; 1 mM DTT; 250 mM sucrose; 0.1% Triton X-100; 1 mM PMSF and 1 tablet complete EDTA-free protease inhibitor (Roche) per 50 ml buffer) and centrifuged for 10 min at 20,000 × g at 4°C. Extracts were then precleared for 30 min against prewashed protein A-Sepharose and the supernatant recovered. The protein concentration was determined by Bradford assays (Biorad) and the protein concentration adjusted to 1 mg/ml. An input aliquot was taken and boiled 15 min with 2x SDS loading buffer. 1 mg extract was then added to equivalent amounts of control and IP antibodies [8 μl rabbit anti-Bic-C or preimmune serum; 12.5 μl mouse anti-GFP (Roche) or mouse IgG] and rotated at 4°C for 2-4 h. To control for RNA dependence, co-immunoprecipitations were performed in the presence of 100 μg/ml RNaseA. Samples were then precipitated with 15 μl of prewashed protein A-Sepharose beads for 1.5 h at 4°C. Beads were then washed three times and bound proteins were eluted by boiling in 50 μl 1.5x SDS loading buffer.

Generation and expression of TAP-Bic-C

To generate the *UASP-TAP-Bic-C* construct, sequences encoding the TAP tag were PCR-amplified from pZOME-N (Cellzome) and subcloned into the *Kpn*I site of *UASP-Bic-C* (Chicoine *et al*., 2007) to produce an in-frame fusion with the *Bic-C* ORF. TAP-Bic-C expression was driven in ovaries using the *nosGal4∴VP16* driver (Van Doren *et al*., 1998).

Genetic interaction assays

For genetic assays, virgin females of the indicated genotypes were collected for three days prior to mating. After two days of mating, egg lays were collected at 4 hr intervals, on three consecutive days and hatching frequencies were scored 48 hr post-collection. All crosses and hatching assays were performed at 25°C.

Acknowledgments

We thank James Wilhelm for the α-Tral antibody and for fly strains. We are also grateful to Akira Nakamura, Norbert Perrimon, the Carnegie FlyTrap collection and FlyBase for fly stocks, to Craig Smibert for α-Cup antibodies, to Richard Mann for the Boca antibody, to Akira Nakamura for antibodies against Rab5, Rab7, Rab11 and Rabenosyn-5, to Thomas Schwarz for α-Sec5, to Uli Tepass for α-Sec8 and to Lucia Cáceres for assistance with fluorescent *in situs*. J.C. was supported by a Fonds pour la Formation de Chercheurs et l'Aide à la Recherche graduate fellowship and a McGill Major award. J.M.K. was supported by a Max Stern Recruitment Fellowship and a McGill Graduate Studies Fellowship. This work was supported by grants to P.L. from the Canadian Cancer Society and from the Canadian Institutes for Health Research.

References

Anderson P, Kedersha N. RNA granules. J Cell Biol 2006;172:803–8. [PubMed: 16520386]

Aspenström P. A Cdc42 target protein with homology to the non-kinase domain of FER has a potential role in regulating the actin cytoskeleton. Curr Biol 1997;7:479–87. [PubMed: 9210375]

Barr FA, Short B. Golgins in the structure and dynamics of the Golgi apparatus. Curr Opin Cell Biol 2003;15:405–13. [PubMed: 12892780]

Beronja S, Laprise P, Papoulas O, Pellikka M, Sisson J, Tepass U. Essential function of *Drosophila* Sec6 in apical exocytosis of epithelial photoreceptor cells. J Cell Biol 2005;169:635–46. [PubMed: 15897260]

Boag PR, Nakamura A, Blackwell TK. A conserved RNA-protein complex component involved in physiological germline apoptosis regulation in *C. elegans*. Development 2005;132:4975–86. [PubMed: 16221731]

Bokel C, Prokop A, Brown NH. Papillote and Piopio: *Drosophila* ZP-domain proteins required for cell adhesion to the apical extracellular matrix and microtubule organization. J Cell Sci 2005;118:633–42. [PubMed: 15657084]

Buszczak M, Paterno S, Lighthouse D, Bachman J, Planck J, Owen S, Skora AD, Nystul TG, Ohlstein B, Allen A, Wilhelm JE, Murphy TD, Levis RW, Matunis E, Srivali N, Hoskins RA, Spradling AC. The Carnegie protein trap library: a versatile tool for *Drosophila* developmental studies. Genetics 2007;175:1505–31. [PubMed: 17194782]

Castagnetti S, Ephrussi A. Orb and a long poly(A) tail are required for efficient *oskar* translation at the posterior pole of the *Drosophila* oocyte. Development 2003;130:835–43. [PubMed: 12538512]

Chicoine J, Benoit P, Gamberi C, Paliouras M, Simonelig M, Lasko P. Bicaudal-C recruits CCR4-NOT deadenylase to target mRNAs and regulates oogenesis, cytoskeletal organization, and its own expression. Dev Cell 2007;13:691–704. [PubMed: 17981137]

Christerson LB, McKearin DM. orb is required for anteroposterior and dorsoventral patterning during *Drosophila* oogenesis. Genes Dev 1994;8:614–28. [PubMed: 7926753]

Culi J, Mann RS. Boca, an endoplasmic reticulum protein required for wingless signaling and trafficking of LDL receptor family members in *Drosophila*. Cell 2003;112:343–54. [PubMed: 12581524]

Forlani S, Ferrandon D, Saget O, Mohier E. A regulatory function for K10 in the establishment of dorsoventral polarity in the *Drosophila* egg and embryo. Mech Dev 1993;41:109–20. [PubMed: 8518190]

Ghiglione C, Bach EA, Paraiso Y, Carraway KL, Noselli S, Perrimon N. Mechanism of activation of the *Drosophila* EGF Receptor by the TGF-α ligand Gurken during oogenesis. Development 2002;129:175–86. [PubMed: 11782411]

Gonzalez-Reyes A, Elliott H, St Johnston D. Polarization of both major body axes in *Drosophila* by Gurken-Torpedo signalling. Nature 1995;375:654–8. [PubMed: 7791898]

Goodrich JS, Clouse KN, Schüpbach T. Hrb27C, Sqd and Otu cooperatively regulate *gurken* RNA localization and mediate nurse cell chromosome dispersion in *Drosophila* oogenesis. Development 2004;131:1949–58. [PubMed: 15056611]

Guichard A, Roark M, Ronshaugen M, Bier E. *brother of rhomboid*, a *rhomboid*-related gene expressed during early *Drosophila* oogenesis, promotes EGF-R/MAPK signaling. Dev Biol 2000;226:255–66. [PubMed: 11023685]

Hawkins NC, Van Buskirk C, Grossniklaus U, Schüpbach T. Post-transcriptional regulation of *gurken* by *encore* is required for axis determination in *Drosophila*. Development 1997;124:4801–10. [PubMed: 9428416]

Herpers B, Rabouille C. mRNA localization and ER-based protein sorting mechanisms dictate the use of transitional endoplasmic reticulum-Golgi units involved in *gurken* transport in *Drosophila* oocytes. Mol Biol Cell 2004;15:5306–17. [PubMed: 15385627]

Kleizen B, Braakman I. Protein folding and quality control in the endoplasmic reticulum. Curr Opin Cell Biol 2004;16:343–9. [PubMed: 15261665]

Kobayashi, S.; Amikura, R.; Nakamura, A.; Lasko, P. Techniques for analyzing protein and RNA distribution in *Drosophila* ovaries and embryos at structural and ultrastructural resolution. In: Richter,

J., editor. Advances in molecular biology: A comparative methods approach to the study of ovaries and embryos. Oxford University Press; Oxford: 1999. p. 426-45.

Lantz V, Chang JS, Horabin JI, Bopp D, Schedl P. The *Drosophila* orb RNA-binding protein is required for the formation of the egg chamber and establishment of polarity. Genes Dev 1994;8:598–613. [PubMed: 7523244]

Lee S, Cooley L. jagunal is required for reorganizing the endoplasmic reticulum during *Drosophila* oogenesis. J Cell Biol 2007;176:941–52. [PubMed: 17389229]

Lighthouse DV, Buszczak M, Spradling AC. New components of the *Drosophila* fusome suggest it plays novel roles in signaling and transport. Dev Biol 2008;317:59–71. [PubMed: 18355804]

Lin MD, Fan SJ, Hsu WS, Chou TB. *Drosophila* decapping protein 1, dDcp1, is a component of the Oskar mRNP complex and directs its posterior localization in the oocyte. Dev Cell 2006;10:601–13. [PubMed: 16678775]

Luna A, Matas OB, Martínez-Menárguez JA, Mato E, Durán JM, Ballesta J, Way M, Egea G. Regulation of protein transport from the Golgi complex to the endoplasmic reticulum by CDC42 and N-WASP. Mol Biol Cell 2002;13:866–79. [PubMed: 11907268]

Mahone M, Saffman EE, Lasko PF. Localized Bicaudal-C RNA encodes a protein containing a KH domain, the RNA binding motif of FMR1. EMBO J 1995;14:2043–55. [PubMed: 7538070]

Murthy M, Schwarz TL. The exocyst component Sec5 is required for membrane traffic and polarity in the *Drosophila* ovary. Development 2004;131:377–88. [PubMed: 14681190]

Nagaso H, Murata T, Day N, Yokoyama KK. Simultaneous detection of RNA and protein by *in situ* hybridization and immunological staining. J Histochem Cytochem 2001;49:1177–82. [PubMed: 11511686]

Nakamura A, Amikura R, Hanyu K, Kobayashi S. Me31B silences translation of oocyte-localizing RNAs through the formation of cytoplasmic RNP complex during *Drosophila* oogenesis. Development 2001;128:3233–42. [PubMed: 11546740]

Nakamura A, Sato K, Hanyu-Nakamura K. *Drosophila* Cup is an eIF4E binding protein that associates with Bruno and regulates *oskar* mRNA translation in oogenesis. Dev Cell 2004;6:69–79. [PubMed: 14723848]

Nakamura T, Hayashi T, Nasu-Nishimura Y, Sakaue F, Morishita Y, Okabe T, Ohwada S, Matsuura K, Akiyama T. PX-RICS mediates ER-to-Golgi transport of the N-cadherin/β-catenin complex. Genes Dev 2008;22:1244–56. [PubMed: 18451111]

Nelson MR, Leidal AM, Smibert CA. *Drosophila* Cup is an eIF4E-binding protein that functions in Smaug-mediated translational repression. Embo J 2004;1:150–59. [PubMed: 14685270]

Neuman-Silberberg FS, Schupbach T. The *Drosophila* dorsoventral patterning gene *gurken* produces a dorsally localized RNA and encodes a TGFα-like protein. Cell 1993;75:165–74. [PubMed: 7691414]

Röper K. Rtnl1 is enriched in a specialized germline ER that associates with ribonucleoprotein granule components. J Cell Sci 2007;120:1081–92. [PubMed: 17327273]

Saffman EE, Styhler S, Rother K, Li W, Richard S, Lasko P. Premature translation of *oskar* in oocytes lacking the RNA-binding protein Bicaudal-C. Mol Cell Biol 1998;18:4855–62. [PubMed: 9671494]

Sambrook, J.; Russell, DW. Molecular Cloning: A Laboratory Manual. Cold Spring Harbor Laboratory Press; New York: 1989.

Stamnes M. Regulating the actin cytoskeleton during vesicular transport. Curr Opin Cell Biol 2002;14:428–33. [PubMed: 12383793]

Tanaka T, Nakamura A. The endocytic pathway acts downstream of Oskar in *Drosophila* germ plasm assembly. Development 2008;135:1107–17. [PubMed: 18272590]

Twombly V, Blackman RK, Jin H, Graff JM, Padgett RW, Gelbart WM. The TGF-β signaling pathway is essential for Drosophila oogenesis. Development 1996;122:1555–65. [PubMed: 8625842]

Van Doren M, Williamson AL, Lehmann R. Regulation of zygotic gene expression in *Drosophila* primordial germ cells. Curr Biol 1998;8:243–6. [PubMed: 9501989]

Weston A, Sommerville J. Xp54 and related (DDX6-like) RNA helicases: roles in messenger RNP assembly, translation regulation and RNA degradation. Nucleic Acids Res 2006;34:3082–94. [PubMed: 16769775]

Wilhelm JE, Buszczak M, Sayles S. Efficient protein trafficking requires Trailer Hitch, a component of a ribonucleoprotein complex localized to the ER in *Drosophila*. Dev Cell 2005;9:675–85. [PubMed: 16256742]

Wilhelm JE, Mansfield J, Hom-Booher N, Wang S, Turck CW, Hazelrigg T, Vale RD. Isolation of a ribonucleoprotein complex involved in mRNA localization in *Drosophila* oocytes. J Cell Biol 2000;148:427–40. [PubMed: 10662770]

Wu WJ, Erickson JW, Lin R, Cerione RA. The γ-subunit of the coatomer complex binds Cdc42 to mediate transformation. Nature 2000;402:800–4. [PubMed: 10866202]

Yang WH, Yu JH, Gulick T, Bloch KD, Bloch DB. RNA-associated protein 55 (RAP55) localizes to mRNA processing bodies and stress granules. RNA 2006;12:547–54. [PubMed: 16484376]

Zhao D, Woolner S, Bownes M. The Mirror transcription factor links signalling pathways in *Drosophila* oogenesis. Dev Genes Evol 2000;210:449–57. [PubMed: 11180850]

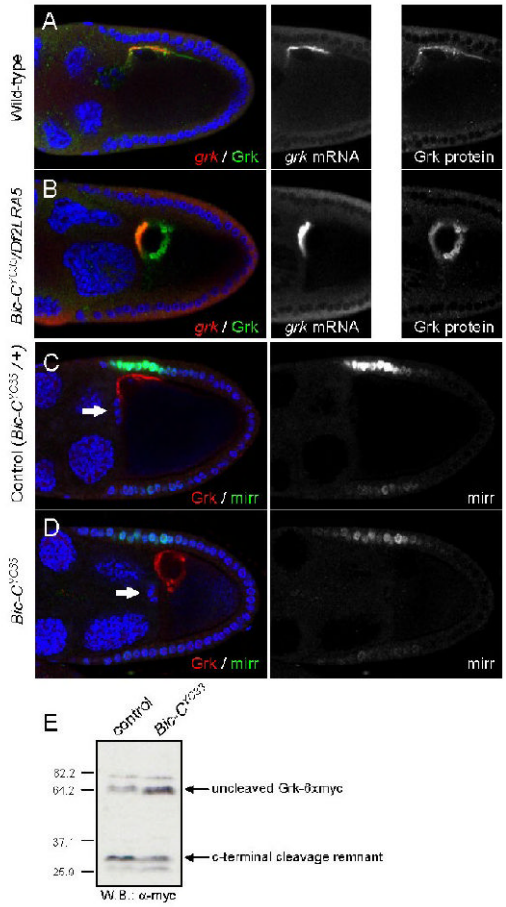

Figure 1. Bic-C is required for normal Grk localization and Egfr activation but not for *grk* mRNA localization

(A-B) Immunofluorescence and fluorescent mRNA *in* situ hybridizations reveal the distribution of Grk protein (green) and *grk* mRNA (red) in wt (A) and Bic-C deficient (B) ovaries. DNA is visualized by DAPI staining (blue). (C-D) Immunofluorescence illustrates Grk protein (red) and β-Gal (representative of Mirr, green) expression in a heterozygous control (C) and a homozygous (D) *Bic-C*^{YC33} mutant. Arrows mark the position of the border cells, indicating that the egg chambers are equivalently staged at late stage 9 or early stage 10A. (E) Western blotting with α-Myc illustrates Grk-(Myc)$_6$ cleavage in ovaries from wt (lane 1) or homozygous *Bic-C*^{YC33} mutant females (lane 2). Molecular weight standards indicate size in kDa.

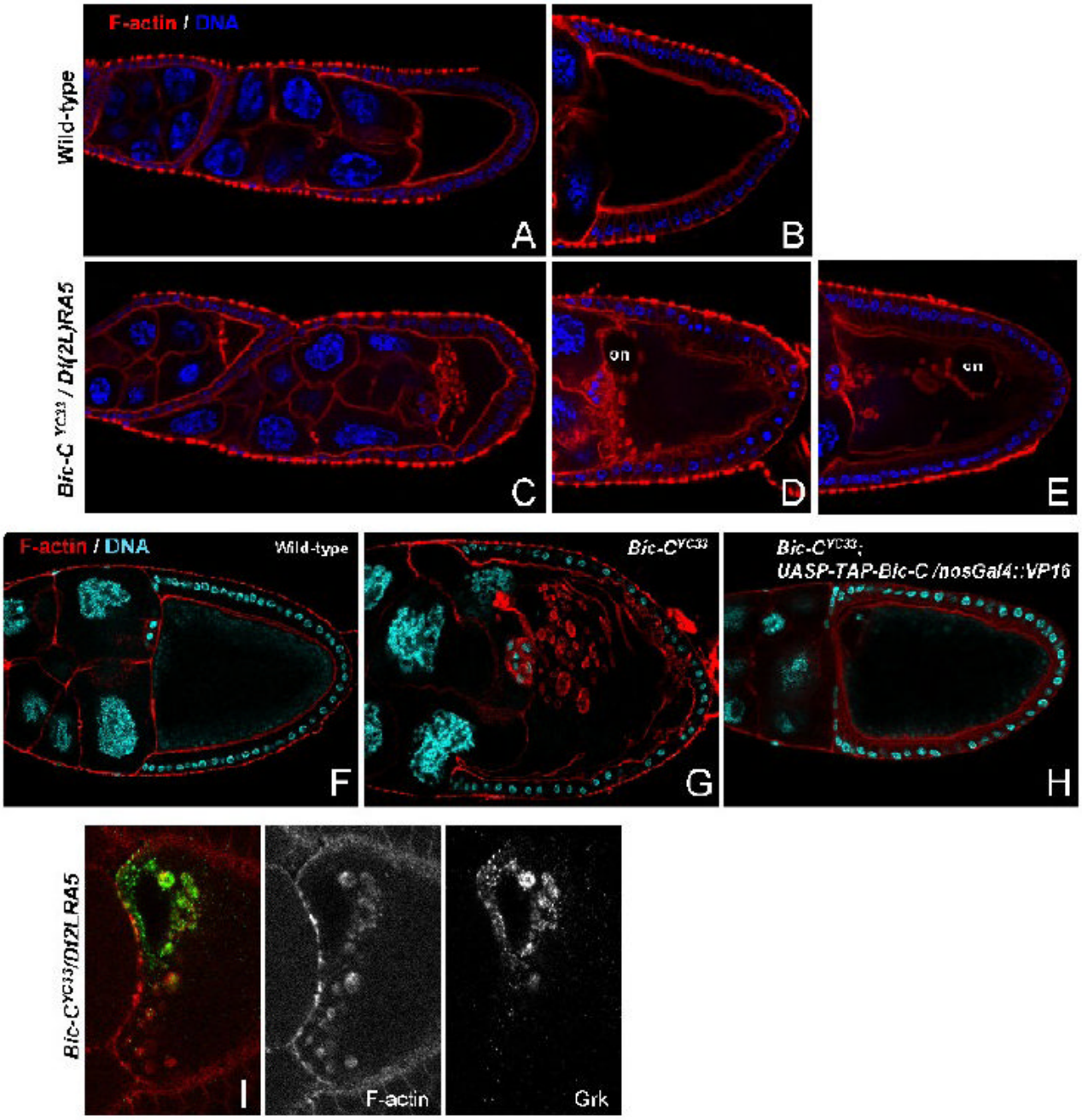

Figure 2. *Bic-C* mutants display defects in actin distribution and form aberrant actin-coated spheres, many of which contain Grk

Phalloidin staining illustrates the normal distribution of F-actin (red) in wt stage 6 and 9 (A) and stage 10 (B) egg chambers. In Bic-C deficient egg chambers, F-actin-coated structures accumulate within the anterior oocyte cytoplasm as early as stage 6 (C) and increase in both size and number through stage 9 (D), until egg chambers start to degenerate at stage 10 (E). Also note that the oocyte cortex is often disorganized (D) and/or separates from the overlying follicle cells (E) and the oocyte nucleus (on) often dissociates from the anterior dorsal cortex. DNA is visualized by DAPI staining (blue). (F-H) DNA and F-actin are visualized by DAPI (blue) and phalloidin (red) staining in wt (F), *Bic-C*^{YC33} homozygotes (G) and *Bic*^{YC33}

homozygotes with germline expression of TAP-Bic-C (H). Note that germline expression of TAP-Bic-C restores centripetal migration of the follicle cells in *Bic*^{YC33} homozygotes at stage 10B and prevents the formation of F-actin-coated aggregates within the oocyte. (I) In Bic-C deficient ovaries, the majority of Grk protein (green) is concentrated within a subset of the F-actin-coated structures (red), located closest to the oocyte nucleus. F-actin spheres further removed from the oocyte nucleus do not contain detectable amounts of Grk.

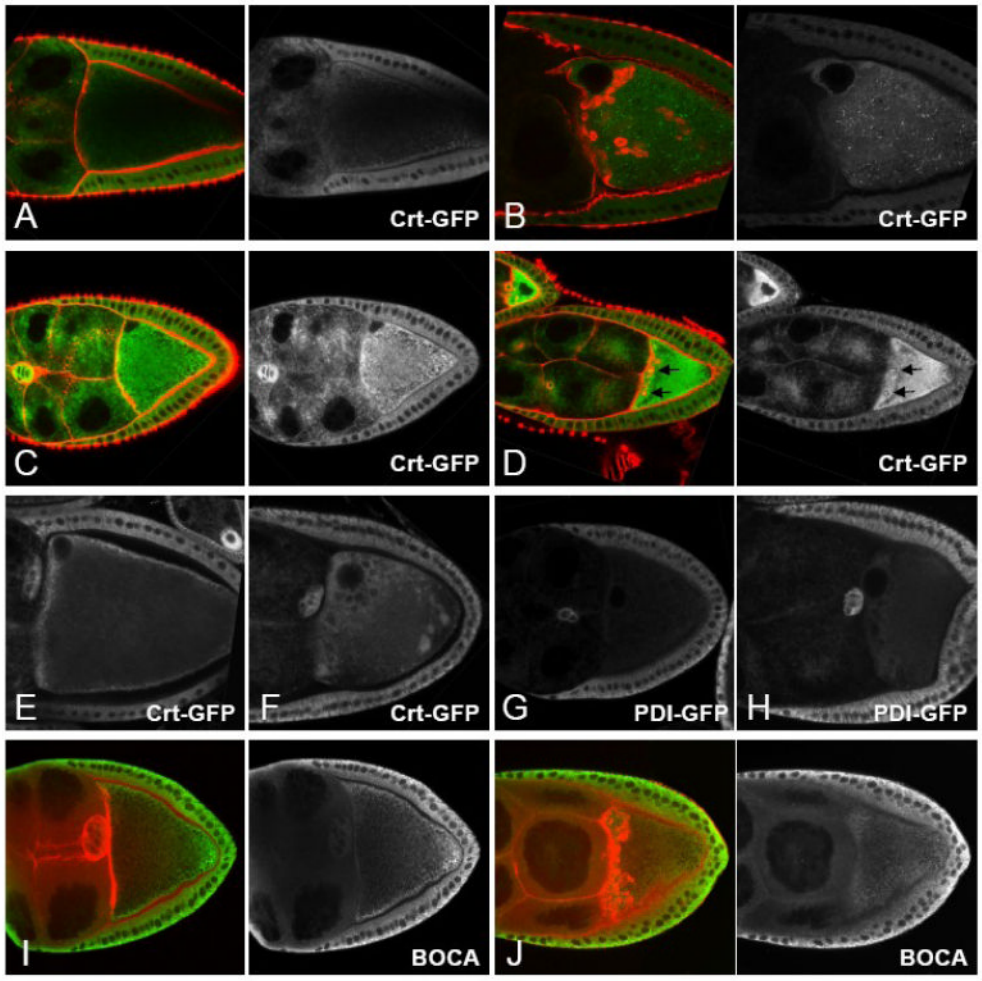

Figure 3. Some ER markers are excluded from the actin-coated spheres in *Bic-C* oocytes

(A-D) Fixed tissue showing the distribution of Crt-GFP (green) and F-actin (red) in *Bic-C*^{YC33}/+ (A, C) and homozygous *Bic-C*^{YC33} mutant (B, D) egg chambers. Crt-GFP is not enriched in F-actin spheres in the *Bic-C* mutant egg chambers during stages 9-10 (B). In younger *Bic-C* oocytes, Crt-GFP is sometimes present inside the actin-coated structures (D, see arrows). (E-H) Live imaged ovaries expressing Crt-GFP (E, F) or PDI-GFP (G, H) in *Bic-C*^{YC33}/+ (E, G) and homozygous *Bic-C*^{YC33} (F, H) mutant ovaries. Both markers are excluded from spheroid structures in the anterior margin and that surround the oocyte nucleus in *Bic-C* mutant oocytes. (I, J) Ovaries from *Bic-C*^{YC33}/+ (I) and homozygous *Bic-C*^{YC33}_females labeled for Boca (green) and F-actin (red). Boca is neither enriched within, or excluded from the actin spheres.

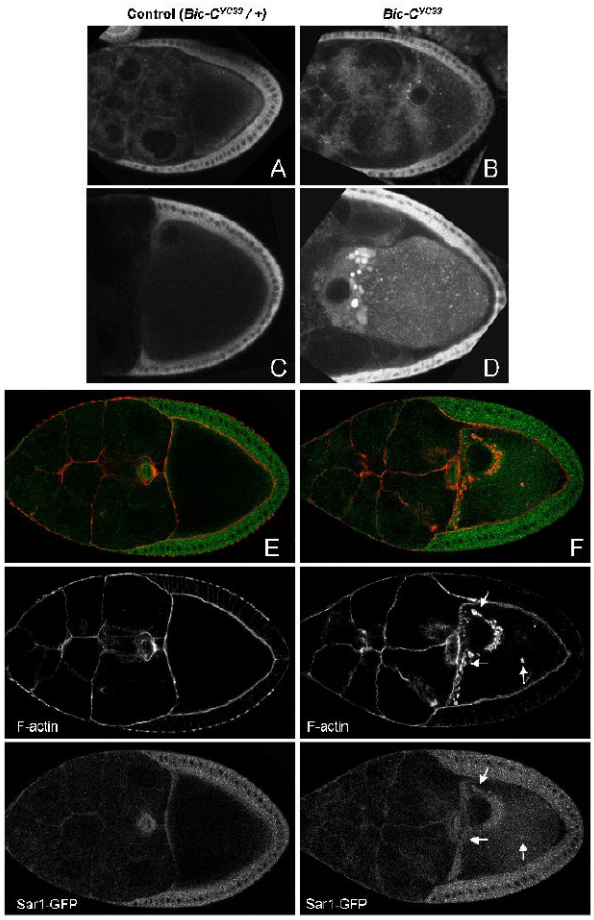

Figure 4. Sar1-GFP accumulates in and around the actin-coated structures in *Bic- C* mutants

Live imaged (A-D) and fixed (E, F) egg chambers expressing Sar1-GFP in a heterozygous (A, C, E) or homozygous *Bic-C*^{YC33} mutant (B, D, F) background. In live imaged homozygous *Bic-C* mutant oocytes, luminous foci of Sar1-GFP accumulate at the anterior of the oocyte. In fixed samples, these foci clearly overlap with the actin-coated structures in *Bic-C* (F, see arrows).

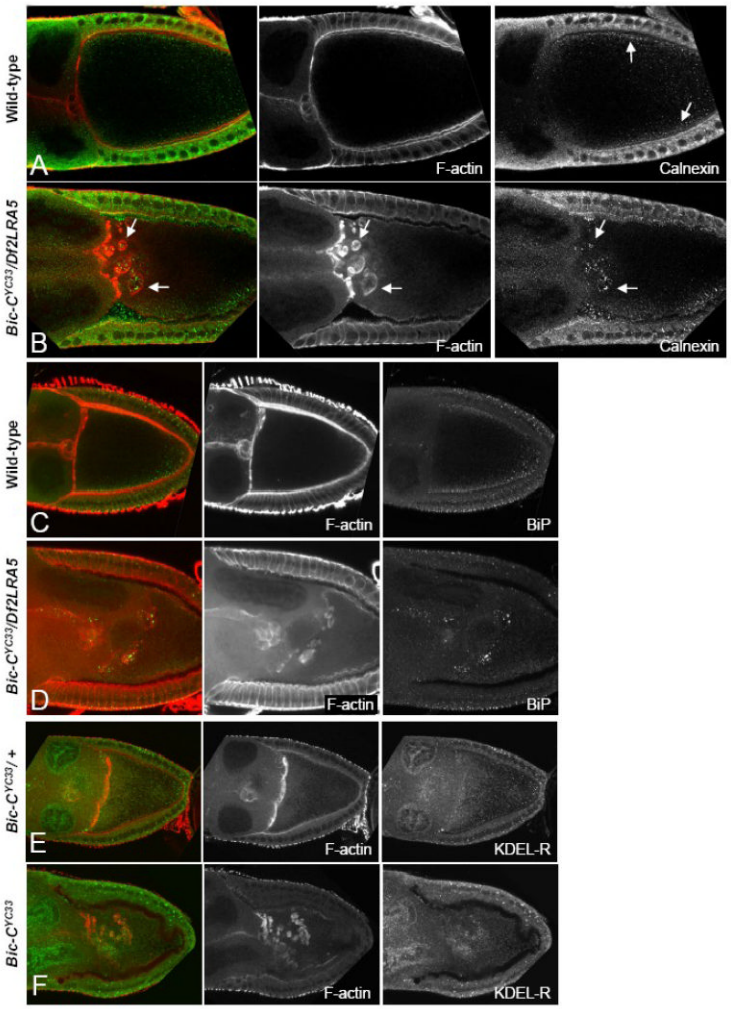

Figure 5. A subset of ER chaperones and the KDEL-receptor accumulate within the actin-coated spheres in *Bic-C* mutant oocytes

(A-B) Immunofluorescent and rhodamine-phalloidin staining illustrates Calnexin (green, see arrows) and F-actin (red) distribution in wt (A) and Bic-C deficient (B) stage 9 egg chambers. (C-D) Fifteen 1 μM confocal sections were merged to illustrate F-actin (red) and BiP (green) distribution in wt (C) and Bic-C deficient (D) egg chambers. (E, F) The KDEL-receptor (green) is located throughout the cytoplasm of heterozygous control (E) and homozygous mutant (F) *Bic-C*^{YC33} stage 8/9 egg chambers. In *Bic-C*^{YC33} homozygotes (F), KDEL-receptor is enriched in the actin-coated structures (red).

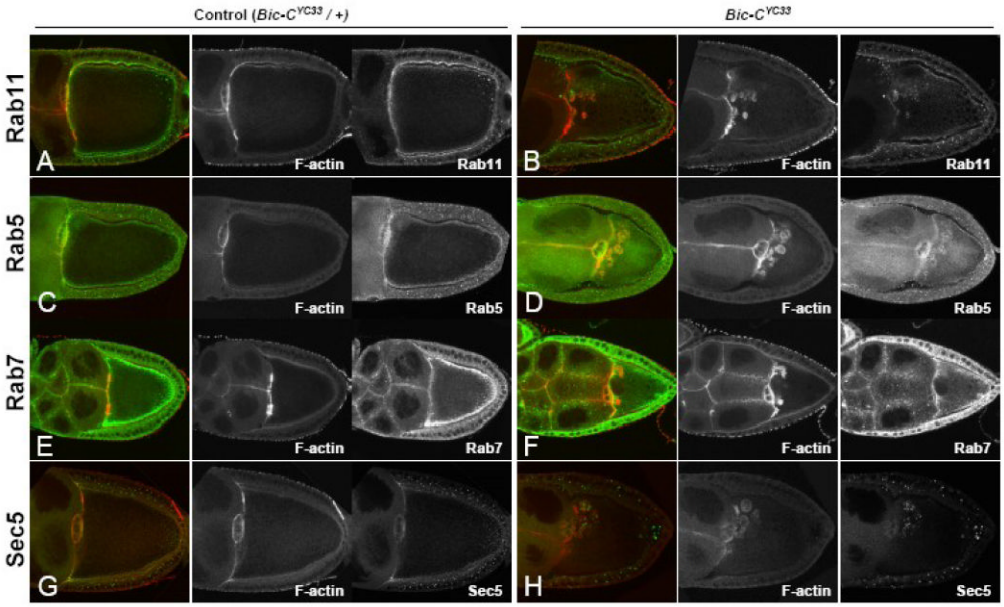

Figure 6. A subset of Rab proteins and the exocyst component Sec5 are enriched in the actin-coated structures in Bic-C mutant oocytes

(A-H) *Bic-C*^{YC33} heterozygous controls (A, C, E, G) and homozygous *Bic-C*^{YC33} egg chambers (B, D, F, H) were stained for F-actin (red) and immuno-stained (green) for: Rab11 (A, B), Rab5 (C, D), Rab7 (E, F), and Sec5 (G, H).

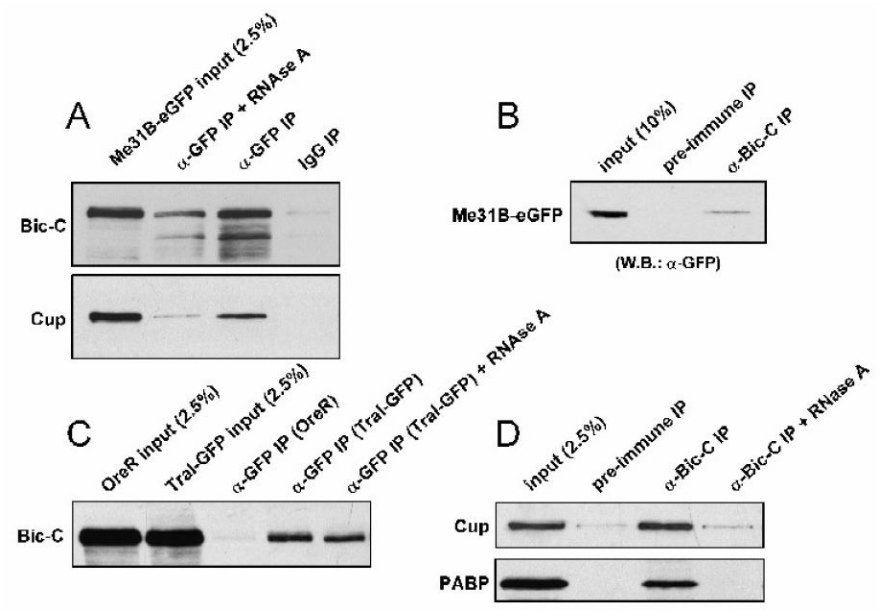

Figure 7. Bic-C associates with multiple components of the Trailer Hitch / Me31B complex

(A) Me31B-eGFP ovarian immune complexes were isolated with α-GFP, while IgG was used as a negative control. Complexes were probed with α-Bic-C (A, top panel) and α-Cup (A, bottom panel). (B) Bic-C immune complexes were isolated from ovaries expressing Me31B-eGFP, while pre-immune sera served as a negative control. Co-precipitating proteins were probed with α-GFP. (C) Tral-GFP was immunoprecipitated with α-GFP from ovarian extracts and co-precipitating proteins were probed with α-Bic-C. An equivalent amount of Oregon-R ovarian extract was used to control for Tral-independent binding. (D) Bic-C immune complexes, isolated from Oregon-R ovarian extracts, were probed with α-Cup (D-Top) and α-PABP (D-Bottom). Pre-immune serum was used as a negative control.

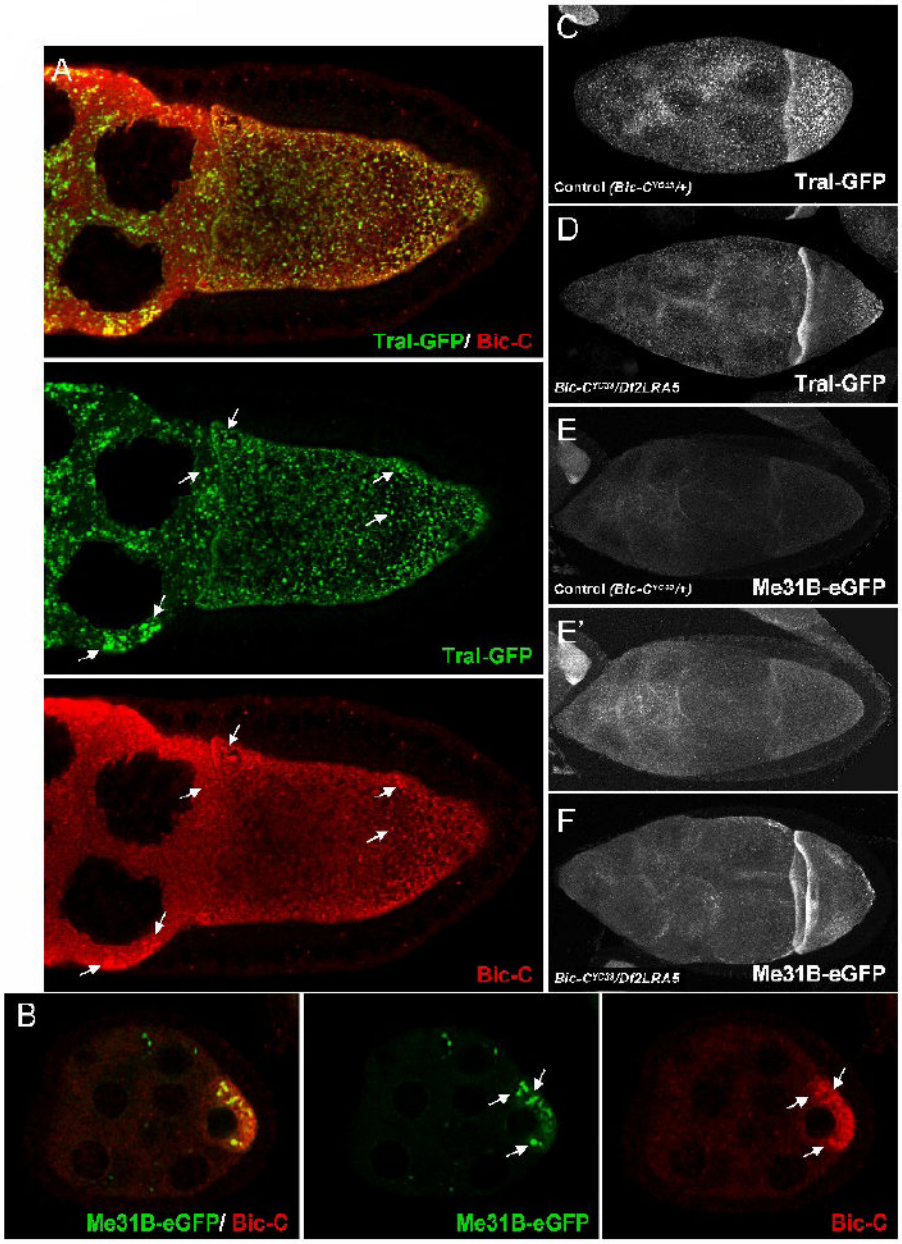

Figure 8. Bic-C co-localizes Tral and Me31B during oogenesis and both proteins are mis-localized in *Bic-C* mutants

Immunofluorescently labeled Bic-C (red) partially co-localizes with Tral-GFP (green) throughout the nurse cell cytoplasm of a late stage 9 /early stage 10 egg chamber (A, see arrows), and with Me31B-eGFP (green) in the oocyte cytoplasm during mid-oogenesis (B, see arrows). Thirty (C, D) or forty (E, F) 1 μM confocal sections were merged to visualize Tral-GFP (C, D) and Me31B-eGFP (E, F) distribution in *Bic-C* heterozygous controls (C, E) and in Bic-C deficient (D, F) fixed stage 8/9 egg chambers. Note that (E) and (F) were taken with identical imaging conditions. (E') is electronically brightened to highlight the difference in Me31B-eGFP distribution in comparison with (F).

Table 1

Embryos derived from *Bic-C cni* transheterozygote females show reduced viability.

Maternal Genotype	n	% Unhatched
+ / *cni(KG00189)*	288	1.0
+ / *cni(1)*	288	4.2
Bic-C(YC33) / +	482	20.1
Bic-C(YC33) / *cni(KG00189)*	900	41.1
Bic-C(YC33) / *cni(1)*	797	61.0

Table 2

Maternal effect lethality in heterozygous *Bic-C* females is dominantly enhanced by a reduction in Trailer Hitch.

Maternal Genotype	n	% Unhatched
tral(1) / +	637	8.2
Df(tral) / +	581	2.7
+ / Bic-C(IIF34)	484	1.7
+ / Bic-C(YC33)	490	3.7
tral(1) / Bic-C(IIF34)	715	19.9
Df(tral) / Bic-C(IIF34)	692	24.2
tral(1) / Bic-C(YC33)	722	29.9
Df(tral) / Bic-C(YC33)	723	23.4